

# Probing the $\beta$ -pocket of the active site of human liver glycogen phosphorylase with 3-(C- $\beta$ -D- glucopyranosyl)-5-(4-substituted-phenyl)-1, 2, 4- triazole inhibitors

Efthimios Kyriakis<sup>1#</sup>, Theodora G.A. Solovou<sup>1#</sup>, Sándor Kun<sup>2</sup>, Katalin Czifrák<sup>2</sup>, Béla Szócs<sup>2</sup>, László Juhász<sup>2</sup>, Éva Bokor<sup>2</sup>, George A. Stravodimos<sup>1</sup>, Anastassia L. Kantsadi<sup>1§</sup>, Demetra S.M. Chatzileontiadou<sup>1§</sup>, Vassiliki T. Skamnaki<sup>1</sup>, László Somsák<sup>2\*</sup>, and Demetres D. Leonidas<sup>1\*</sup>

<sup>1</sup>*Department of Biochemistry and Biotechnology, University of Thessaly, Biopolis, 41500 Larissa, Greece,* <sup>2</sup>*Department of Organic Chemistry, University of Debrecen, POB 400, H-4002 Debrecen, Hungary,*

\*Corresponding authors:

Prof. Demetres D. Leonidas, Department of Biochemistry and Biotechnology, University of Thessaly, Biopolis, 41500 Larissa, Greece. Phone: +30 2410 565278; Fax: +30 2410 565290; e-mail: ddleonidas@bio.uth.gr; Prof. László Somsák, Department of Organic Chemistry, University of Debrecen, POB 400, H-4002 Debrecen, Hungary. Phone: +36 52512900/ext 22348; Fax: +36 52512744; e-mail: somsak@tigris.unideb.hu.

§Present address: Department of Biochemistry, University of Oxford, South Parks Road, Oxford OX1 3QU, U.K.

§Present address: Department of Biochemistry and Molecular Biology, Biomedicine Discovery Institute, Monash University, Clayton, Victoria 3800, Australia.

#Equal contribution

## Abstract

Human liver glycogen phosphorylase (hGP), a key enzyme in glycogen metabolism, is a valid pharmaceutical target for the development of new anti-hyperglycaemic agents for type 2 diabetes. Inhibitor discovery studies have focused on the active site and in particular on glucopyranose based compounds with a  $\beta$ -1 substituent long enough to exploit interactions with a cavity adjacent to the active site, termed the  $\beta$ -pocket. Recently, C- $\beta$ -D-glucopyranosyl imidazoles and 1, 2, 4-triazoles proved to be the best known glucose derived inhibitors of hGP. Here we probe the  $\beta$ -pocket by studying the inhibitory effect of six different groups at the *para* position of 3-( $\beta$ -D-glucopyranosyl phenyl)-5-phenyl-, 1, 2, 4-triazoles in hGP by kinetics and X-ray crystallography. The most bioactive compound was the one with an amine substituent to show a  $K_i$  value of 0.43  $\mu$ M. Structural studies have revealed the physicochemical diversity of the  $\beta$ -pocket providing information for future rational inhibitor design studies.

**Keywords:** glycogen metabolism; diabetes type 2; inhibitor; glycogen phosphorylase; X-ray crystallography; C-glucopyranosyl derivative; 1, 2, 4-triazole.

## 1. Introduction

Type 2 Diabetes mellitus (T2D) is one of the most common and serious metabolic disorders. The number of patients with T2D keeps rising and even exceeds the predictions. It was estimated that in 2015, 415 million of people lived with diabetes all around the world, while approximately 193 million were undiagnosed. This number may increase to 642 million in 2040 according to the International Diabetes Federation (IDF). IDF estimated that diabetes was the primary cause of death to almost 5 million people in 2015 [2]. The pharmaceutical recommendations for T2D thus far, include drugs as metformin (a biguanide drug), aiming at optimizing insulin-mediated glucose uptake from the cells and, therefore, leading to lower blood glucose levels [3]. However, in T2D patients a significant  $\beta$ -cell insulin secretory dysfunction and decreased  $\beta$ -cell mass due to increased apoptosis, are observed. As a result, the body can't handle increases in metabolic load [4] and oral medication shows often limited or even insufficient results. Furthermore, some of these treatments may have side effects, like hypoglycaemia, which affects the quality of diabetic patients' life. Therefore, the identification of new compounds that could result in a better management of blood glucose levels is in need. Hepatic enzymes involved in glycogen metabolism are promising targets for T2D treatment and glycogen phosphorylase (GP; EC 2.4.1.1) inhibitors (GPi's) are confirmed to be able to lead to a better hepatic glycogen balance and blood glucose levels control [5]. These results are supported by *in vitro*, *ex vivo* and *in vivo* studies [6-13]. Furthermore, although GPi's exert their action in the liver, they have also been found to induce UCP2 (a mitochondrial inner membrane protein that uncouples mitochondrial proton gradient from ATP production) expression to protect from mitochondrial hydroxyl radicals produced by excess glucose flux [13]. This has also been observed in the muscle [14, 15]. Recently, Nagy et al, suggested that GPi's can also target pancreatic cells and hence they can improve  $\beta$ -cell function and survival [16].

GP is a key enzyme involved in glycogen metabolism by catalyzing the first step of glycogen breakdown towards glucose-1-phosphate (Glc-1-P). GP has at least seven binding sites: the catalytic, allosteric, inhibitor, quercetin, new allosteric, benzamidazole and the glycogen storage binding

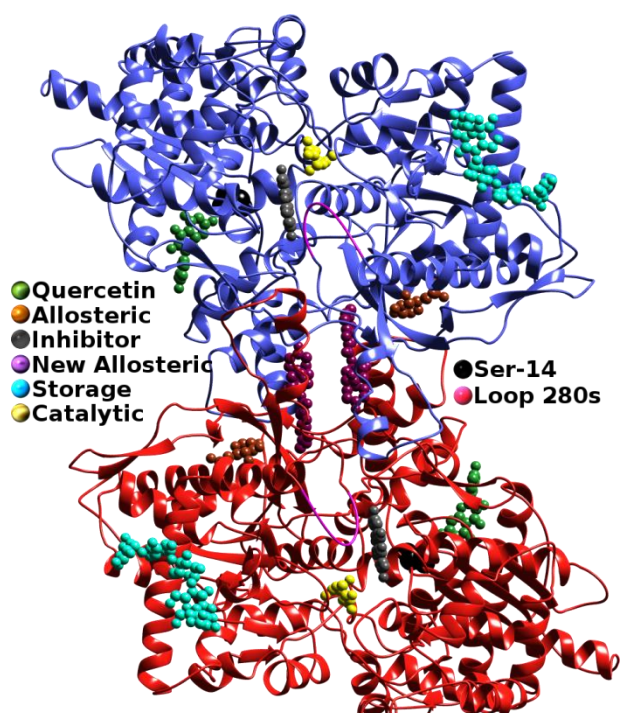


**Figure 1.** The biologically active homodimer of GP in the T-state conformation with the different binding sites [1].

site [11], as shown in Figure 1. GP follows the Monod-Wyman-Changeux model of allosteric enzymes and exists in two forms, GPb with low activity and affinity for the substrate (T-state) and GPa with high activity and affinity for the substrate (R-state). The equilibrium between T and R state lies on a flexible loop (280s, residues 282-286) and is controlled by small molecules (metabolite effectors) that bind on the aforementioned binding sites of the enzyme. The T state is inactive and the substrate cannot reach the catalytic site since it is blocked by the 280s loop. During the allosteric transition from T to R state, the 280s loop is displaced and the catalytic site becomes accessible. The biologically active GP is a homodimer and exists in three isoforms, liver (lGP), brain (bGP) and muscle (mGP), depending on the tissue they are expressed. These isoenzymes share approximately 80-83 % sequence homology, with no insertions or deletions, and there are no structural differences at the catalytic sites of lGP and mGP.

In the past years structure-based inhibitor design studies have led to the discovery of new inhibitors with high affinity for specific GP binding sites. Most studies focused on the active site using glucose derivatives [1, 9, 11]. Recently *C*- $\beta$ -D-glucopyranosyl imidazoles [17] and 1,2,4-triazoles [18] have been studied for their potency against the pharmacologically relevant isoform, human liver

GP (hIGP), revealing the best known glucose derived inhibitors thus far, with  $K_i$  values in the low nM range [17]. The efficiency of these glucose derivatives as GPi's has been attributed to the exploitation of an extensive network of polar and non-polar interactions with residues that form the  $\beta$ -pocket within the catalytic site, so called because only the  $\beta$ -anomeric substituents of D-glucose can bind there. This cavity extends by the catalytic site and inhibitors binding at this site can form an extensive network of interactions with Asp283, Phe285, and Phe286 on one side and Asp339, His341, and Arg292 on the other side [19]. Our recent discovery [18] showed that 3-(C- $\beta$ -D-glucopyranosyl)-5-phenyl-1,2,4-triazole's ( $K_i=156$  nM) and 3-(C- $\beta$ -D-glucopyranosyl)-5-(4-methylphenyl)-1,2,4-triazole's ( $K_i=278$  nM) significant potency was attributed to their extensive van der Waals interactions within the  $\beta$ -pocket. Herein we probe this pocket's characteristics by studying the effect on the inhibitory potency of six groups (-COO<sup>-</sup>, -CF<sub>3</sub>, -NO<sub>2</sub>, -OCH<sub>3</sub>, -OH and -NH<sub>2</sub>), different in size and polarity, in the *para* position of the phenyl group. Moreover, we have determined and analyzed the X-ray crystal structures of their GP-complexes to elucidate their protein binding pattern. We also present a new efficient protocol for the production of sufficient amounts of recombinant human liver GP, which are essential for inhibitor binding studies.

## 2. Materials and Methods

The investigated compounds were synthesized and chemically characterized as described previously [20].

### 2.1 Protein production and purification

Rabbit muscle GPb (rmGPb) was purified from rabbit skeletal muscle following the protocol developed by Fischer & Krebs [21] with a slight modification (L-cysteine was replaced with 2-mercaptoethanol) [22]. The optimized gene sequence encoding human liver glycogen phosphorylase (hIGPa, optimized by Eurofins Genomics, Ebersberg, Germany) was cloned on a pET-M11 vector. The N-terminus site was followed by a His-tag (6xHis) and a TEV protease precission site. The *E. coli* BL21-GOLD (DE3) strain was the host strain for the heterologous protein expression.

Large cultures were produced by inoculating 1 L of LB broth (plus 20  $\mu\text{g}/\text{mL}$  kanamycin, 100 mg/L pyridoxine, and 600 mg/L  $\text{MnCl}_2$ ) with 10 mL overnight cultures (growth in the same conditions). Cultures were grown until reaching  $\text{OD}_{600}$ : 0.5-0.6, at 37°C, 210 rpm and then protein expression was induced using 0.5 mM IPTG. Cultures were incubated for a further 16 hours at 18 °C, 210 rpm. Bacterial cells were harvested with centrifugation and the pellet was resuspended in lysis buffer containing 20 mM  $\beta$ -glycerol phosphate pH 7.0, 500 mM NaCl, 20 mM Imidazole and protease inhibitor cocktail (Roche). The mixture was incubated at 4 °C, for 15 min in the presence of benzonase and then sonicated at 70 % amplitude, 4 °C for total 3 min. Finally, the lysate was centrifuged and the supernatant containing the soluble protein was filtered through a 0.45  $\mu\text{m}$  filter and purified using IMAC (HiTrap Talon Crude, GE Healthcare) and Ion exchange (Resource Q, GE Healthcare) chromatography, applied on ÄKTA purifier (GE Healthcare). The chelating sepharose resin was equilibrated with buffer A (20 mM  $\beta$ -glycerol phosphate pH 7.0, 500 mM NaCl, 20 mM imidazole) before the addition of the crude extract. The column was washed with buffer A and then the protein eluted with buffer B (20 mM  $\beta$ -glycerol phosphate pH 7.0, 500 mM NaCl, 500 mM imidazole) followed by overnight dialysis against a buffer containing 20 mM Tris HCl pH 8.0 and 1 mM DTT using dialysis tubing (10 kDa MWCO, Sigma). The protein was then loaded on an anion exchange column (Resource Q, GE Healthcare) which was pre-equilibrated in buffer A (20 mM Tris HCl pH 8.0, 1 mM DTT). The column was washed with buffer A and the protein eluted with gradient concentration of buffer B (20 mM Tris HCl pH 8.0, 1 mM DTT, 1 M NaCl). Afterwards the protein incubated overnight in presence of TEV protease (His-tagged) at 4 °C for 16 hours. TEV protease and the uncleaved protein were separated, applying a HiTrap Talon Crude (GE Healthcare) column, from the cleaved protein which was collected (flow through) and concentrated. This procedure led to 250  $\mu\text{g}$  of pure hIGPb sample per Lt of bacterial culture based on SDS-PAGE. Phosphorylation of rmGPb and hIGPb was performed using a truncated form of the  $\gamma$  (catalytic) subunit of rabbit skeletal muscle phosphorylase kinase as described previously [17].

## 2.2 Kinetic studies

GP's catalytic activity is reversible *in vitro*, with ratio of [Glc-1-P]/[Pi] to 0.22. *In vivo* the enzyme catalyzes only the degradation of glycogen since Pi concentration is much higher than Glc-1-P's. *In vitro*, GP can perform the reverse reaction in presence of higher concentrations of Glc-1-P, where the enzyme adds glucose residues on glycogen with direct release of Pi which is measured spectrophotometrically using the method Shaheki et al. [23]. Kinetic studies were performed at 30 °C in the direction of glycogen synthesis. 3 µg/ml rmGPb, rmGPa, or 1 µg/mL hGPa were assayed in a 30 mM imidazole/HCl buffer (pH 6.8) containing 60 mM KCl, 0.6 mM EDTA, and 0.6 mM dithiothreitol using constant concentrations of glycogen (0.2% w/v), AMP (1 mM; only for the rmGPb experiments), and various concentrations of Glc-1-P and inhibitors. Enzyme and glycogen were pre-incubated for 15 min at 30 °C before initiating the reaction with Glc-1-P. Initial velocities were calculated from the pseudo-first order rate constants using five time-intervals. For the calculation and statistical evaluation of the kinetic parameters, the non-linear regression program Grafit [24] was used.

### 2.3 X-ray crystallography

rmGPb-inhibitor complexes were formed by diffusion of 10 mM solution of the inhibitors in the crystallization media supplemented with DMSO (15 %, v/v) in preformed rmGPb crystals at room temperature for 3 hours prior to data collection. Tetragonal T state rmGPb crystals were grown as described previously [25]. These crystals belong to space group P4<sub>3</sub>2<sub>1</sub>2 with unit cell dimensions a=b=128.5 Å and c=116.2 Å. X-ray diffraction data were collected using synchrotron radiation on station ID911-2 ( $\lambda=1.0403\text{\AA}$ ) at MAX-Lab Synchrotron Radiation Source in Lund, Sweden at room temperature on a MAR CCD detector 165 mm. To avoid crystal radiation damage the crystal was translated five times. Crystal orientation, integration of reflections, inter-frame scaling, partial reflection summation, and data reduction was performed by the program Mosflm [26]. Scaling and merging of intensities were performed by Aimless [27] and the optimum resolution was selected based on the  $CC^{1/2}$  criterion [28]. Crystallographic refinement of the complexes was performed by maximum-likelihood methods using REFMAC [29]. The starting model employed for the refine-

ment of the complexes was the structure of the native T state rmGPb complex determined at 1.9 Å resolution (Leonidas et al., unpublished results). Ligand molecule coordinates and topologies were constructed using JLigand [30] and they were fitted to the electron density maps by adjusting of their torsion angles. Alternate cycles of manual rebuilding with the molecular graphic program COOT [31] and refinement with REFMAC improved the quality of the models. A summary of the data processing and refinement statistics for the inhibitor complex structures is given in Table 1 and the validity of the refinement procedure was checked using the PDB\_REDO server [32]. As there were more than 5 reflections per atom available, both an isotropic and an anisotropic B-factor model were considered, and the isotropic B-factor model was selected based on the Hamilton R ratio test. A TLS model for grouped atom movement with one TLS group was used. The stereochemistry of the protein residues was validated by MolProbity [33]. Hydrogen bonds and van der Waals interactions were calculated with the program CONTACT as implemented in CCP4 [34] applying a distance cut off 4.1 Å (details are provided in Table 3) and 4.0 Å, respectively. Figures were prepared with CCP4 Molecular Graphics [35]. The coordinates of the new structures have been deposited with the RCSB Protein Data Bank (<http://www.rcsb.org/pdb>) with codes presented in Table 1.



<b>Table 1:</b> Summary of the diffraction data processing and refinement statistics for the GPb complexes. Values in parentheses are for the outermost shell.						
<b>GPb complex</b>	<b>KS252</b>	<b>JLH270</b>	<b>CK898</b>	<b>CK900</b>	<b>SzB102v</b>	<b>KS172</b>
<i>Data Processing and collection statistics</i>						
Resolution (Å)	38.7-1.9 (2.0-1.9)	38.4-1.85 (1.95- 1.85)	38.75-1.9 (2.0-1.9)	38.4-1.8 (1.9-1.8)	38.4-1.9 (2.0-1.9)	38.4-1.85 (1.95-1.85)
Reflections measured	353099	271775	300822	230851	251878	329820
Unique reflections	74613 (10693)	80695 (11707)	75574 (10787)	87453 (12453)	72951 (10736)	80615 (11668)
$R_{\text{merge}}$	0.069 (0.481)	0.063 (0.430)	0.057 (0.318)	0.053 (0.492)	0.064 (0.425)	0.056 (0.396)
Completeness (%)	97.7 (97.1)	97.3 (97.4)	98.5 (97.6)	97.5 (96.2)	95.8 (97.2)	97.4 (97.3)
$\langle I/\sigma(I) \rangle$	13.6 (3.4)	11.2 (2.8)	14.0 (4.0)	10.2 (2.0)	12.2 (3.2)	12.9 (3.3)
Multiplicity	4.7 (4.8)	3.4 (3.3)	4.0 (4.0)	2.6 (2.6)	3.5 (3.4)	4.1 (4.1)
$CC^{1/2}$	0.997 (0.776)	0.996 (0.738)	0.997 (0.889)	0.997 (0.713)	0.836 (0.739)	0.996 (0.903)
B Wilson (Å <sup>2</sup> )	23.2	23.0	26.3	28.2	22.1	23.4
Reflections used for refinement	70859	76693	71701	83063	69283	76620
No of water molecules	292	304	294	316	304	293
No of ligand atoms	72	52	79	70	70	73
$R$ ( $R_{\text{free}}$ ) (%)	17.2 (19.7)	16.7 (19.6)	16.5 (19.9)	16.3 (19.1)	16.5 (19.7)	14.9 (18.7)
Outer shell $R$ ( $R_{\text{free}}$ ) (%)	25.8 (28.3)	26.5 (26.7)	24.2 (30.4)	27.8 (30.3)	25.8 (29.8)	24.0 (26.6)
r.m.s.d. in bond lengths (Å)	0.009	0.010	0.010	0.010	0.010	0.020
r.m.s.d. in bond angles (°)	1.3	1.3	1.4	1.4	1.4	1.9
<i>Average B (Å<sup>2</sup>)</i>						
Protein atoms	29.7	31.0	33.2	32.4	29.8	33.0
Water molecules	35.5	37.0	38.8	37.8	35.6	37.1
Ligand atoms	30.7	23.8	41.5	40.9	30.2	39.4
PDB entry	5OWY	5OX1	5OX0	5OX4	5OX3	5OWZ

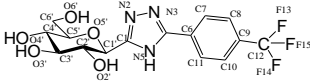
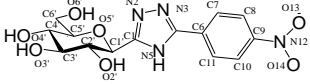
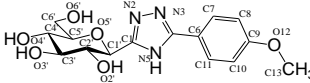
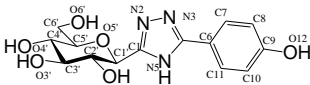
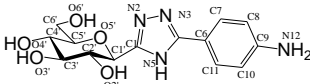
### 3. Results and Discussion

#### 3.1 Kinetic studies

In order to evaluate the inhibitory potency of our six different compounds we determined their inhibitor constants ( $K_i$ ) against hlGPa with kinetic experiments as described above. Kinetic experiments were also performed against rmGPa for comparison reasons (liver and muscle) and with rmGPb to validate the structural data (see below). Results are summarized in Table 2, together with three other similar derivatives [18]. All of the compounds displayed competitive inhibition with respect to the substrate Glc-1-P as revealed by the Lineweaver-Burk plots that intersect at the same point on the y-axis for hlGPa and rmGPa. The  $K_i$  values, derived from the  $1/v$  vs  $[I]$  plots, do not display any significant differences between rmGPb, rmGPa and hlGPa as found earlier [17, 18]. The most potent compound is **CK900** with a  $K_i$  value at  $0.427 \mu\text{M}$  and a  $-\text{NH}_2$  substituent. All substituents seem to have a significant impact on the inhibitory potency of hlGPa and their  $K_i$  values follow the pattern  $-\text{COO}^- > \text{CF}_3 > -\text{NO}_2 > -\text{OCH}_3 > -\text{OH} > -\text{NH}_2$ . From this classification it seems that the most influential characteristic of the substituents to the inhibitory potency is their size rather than their polarity, the presence of hydrogen bond donors/acceptors, or the presence/absence of acid/base properties. This notion is further supported by previous results [18] whereas **2d**, with  $-\text{CH}_3$  group displays a  $K_i$  value at  $0.283 \mu\text{M}$  (Table 2). However, comparing the  $K_i$  value of **2d**, with that of **KS172** it seems that increasing hydrophilicity by replacing hydrogens with fluorine leads to a drop in the inhibitory potency by 195 times. Furthermore it seems that all compounds show similar potency against all three enzymes and do not display a preference for any of them.

**Table 2 :** The chemical structures of the studied inhibitors with the  $K_i$  values and the crystallographic numbering

Compound	Chemical structure	$K_i$ ( $\mu\text{M}$ )		
		hlGPa	rmGPa	rmGPb
<b>2a</b>		1.35 [18]	1.74 [18]	7 [20]
<b>2d</b>		0.283 [18]	0.283 [18]	1.7 [20]
<b>2b</b>		0.172 [18]	0.172 [18]	0.411 [20]
<b>KS252</b>		$637.41 \pm 32.67$	$660 \pm 55.03$	No inh. at 625

<b>KS172</b>		$55.3 \pm 0.8$	$36.3 \pm 2.0$	111
<b>CK898</b>		$32.70 \pm 1.85$	$10.00 \pm 0.46$	33.5
<b>JLH270</b>		$5.25 \pm 0.23$	$3.39 \pm 0.23$	1.95
<b>SzB102v</b>		$3.66 \pm 0.15$	$3.51 \pm 0.13$	2.9
<b>CK900</b>		$0.427 \pm 0.011$	$0.550 \pm 0.047$	0.67

### 3.2 Structural studies

The active sites, the  $\beta$ -pockets and the flexible 280s loop in hIGP and rmGP are almost identical (Fig. 2) in terms of sequence and structure (the r.m.s.d. between the two structures is 1.0 Å over well-defined residues (18–49, 262–312, 326–829). Thus structural data with rmGPb can be directly correlated with hIGP. To elucidate the structural basis for the differences in the inhibitory potency of the six inhibitors, we have determined the crystal structures of the rmGPb-inhibitor complexes. The 2Fo-Fc and Fo-Fc electron density maps revealed that all six inhibitors were bound at the active site and clearly defined the position of each atom of the ligands (Fig. 3). The superposition of the structures of free rmGPb and the rmGPb-inhibitor complexes over well-defined residues (18–49, 262–312, 326–829) gave r.m.s.d. values of 0.111, 0.125, 0.141, 0.122, 0.120, and 0.122 Å for the **KS252**, **KS172**, **CK898**, **JLH270**, **SzB102v**, **CK900** complexes, respectively, indicating that the binding of the inhibitors at the catalytic site did not trigger any major conformational change on the overall protein structure.

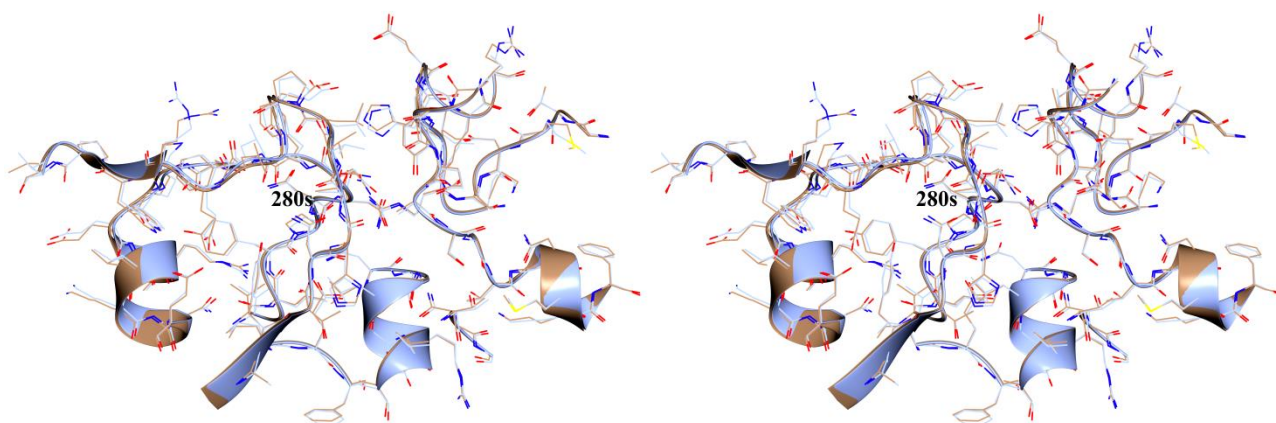


**Figure 2.** A stereo diagram of the superposition of the rmGPb-CK900 complex structure (brown) onto the hGPa-N-acetyl- $\beta$ -D-glucopyranosylamine complex structure [36] in blue, at the active site including the 280s loop (labelled 280s) and the  $\beta$ -pocket. The inhibitor molecules have been omitted for clarity.

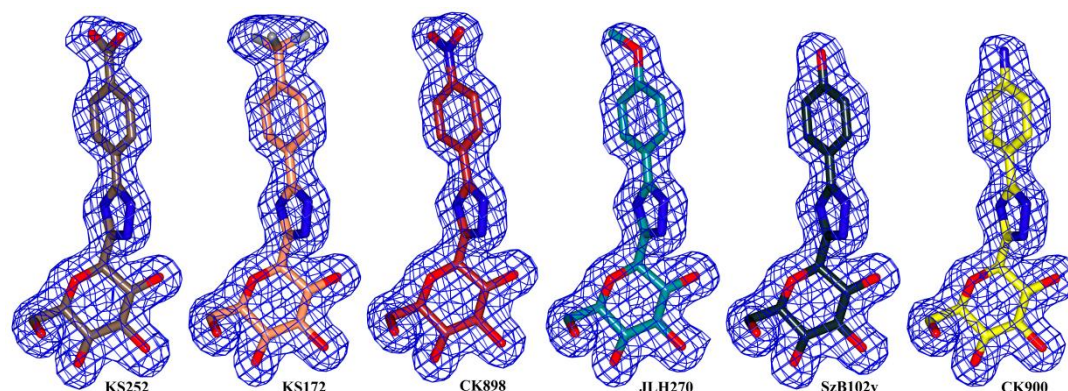


**Figure 3.** The REFMAC weighted 2Fo-Fc electron density maps of the bound ligands at the catalytic site contoured at 1.0  $\sigma$  before the incorporation of the ligand molecules in the refinement process. The final models of the inhibitors are also shown.

The anchor point for each of the inhibitors at the catalytic site appears to be the glucose moiety which is engaged in hydrogen bond (Table 3) and van der Waals interactions almost identical to those that have been observed for  $\alpha$ -D-glucose and other glucose-based inhibitors in previous studies [9, 17, 18, 37-39]. Furthermore, three conserved water molecules mediate hydrogen bond interactions between the glucopyranose moiety of each ligand and residues Asn284, Asp283, Ala673, Lys574, Thr671, Gly675, Thr676, and the phosphate group of the cofactor PLP.

---

**Table 3.** Potential hydrogen bond interactions of inhibitors with rmGPb residues at the catalytic site in the crystal. Numbers shown are distances in Å. Hydrogen bonds are reported if the distance is less than 4.1 Å and the angle at the donor group is above 100°.

---

Inhibitor atoms	Protein atoms	KS252	KS172	CK898	JLH270	SzB102v	CK900	
<b>Glucopyranose atoms</b>	<b>O2'</b>	Asn284 (ND2)	3.0	3.0	2.7	2.9	2.9	3.0
		Tyr573 (OH)	3.0	3.0	3.0	3.0	3.1	3.0
		Glu672 (OE1)	3.2	3.1	3.2	3.1	3.2	3.2
	<b>O3'</b>	Glu672 (OE2)	2.8	2.7	2.7	2.7	2.8	2.8
		Ala673 (N)	3.3	3.1	3.2	3.2	3.2	3.2
		Ser674 (N)	3.0	3.0	3.1	3.1	3.0	3.0
		Gly675 (N)	3.1	3.1	3.2	3.1	3.1	3.1
	<b>O4'</b>	Gly675 (N)	2.9	2.9	2.9	2.8	2.9	2.9
	<b>O6'</b>	His377 (ND1)	2.7	2.7	2.7	2.7	2.7	2.7
		Asn484 (ND2)	2.8	2.8	2.8	2.8	2.8	2.8
<b>Triazole atoms</b>	<b>N2</b>	His377 (O)	2.8	2.8	2.6	2.8	2.7	2.7
	<b>N5</b>	Asn284 (ND2)	-	-	-	-	-	3.2
<i>para</i> group atoms	<b>O13</b>	Arg292 (NH2)	-	-	3.3	-	-	-
	<b>F13</b>	Arg292 (NH2)	-	3.2	-	-	-	-
	<b>F14</b>	Asn282 (O)	-	3.3	-	-	-	-
		Phe285 (O)	-	2.8	-	-	-	-
	<b>F15</b>	Asn282 (O)	-	3.1	-	-	-	-
<b>Total number of interactions</b>		<b>11</b>	<b>15</b>	<b>12</b>	<b>11</b>	<b>11</b>	<b>12</b>	

The triazole linker participates in a hydrogen bond interaction with the main chain oxygen of His377 (Table 3; Figure 4). Similar interactions have been previously observed with other glucose derivatives studied as GPIs [17, 18, 40-43] and the increased inhibitory potency of these compounds was ascribed to the hydrogen-bond forming capacity of the heterocyclic nitrogen atoms to the main chain oxygen of His377. In addition, the triazole linker of all inhibitors participates in water mediated hydrogen bond interactions with the side chain atoms of Asp283 and the main atoms of Leu136 (Figure 4).

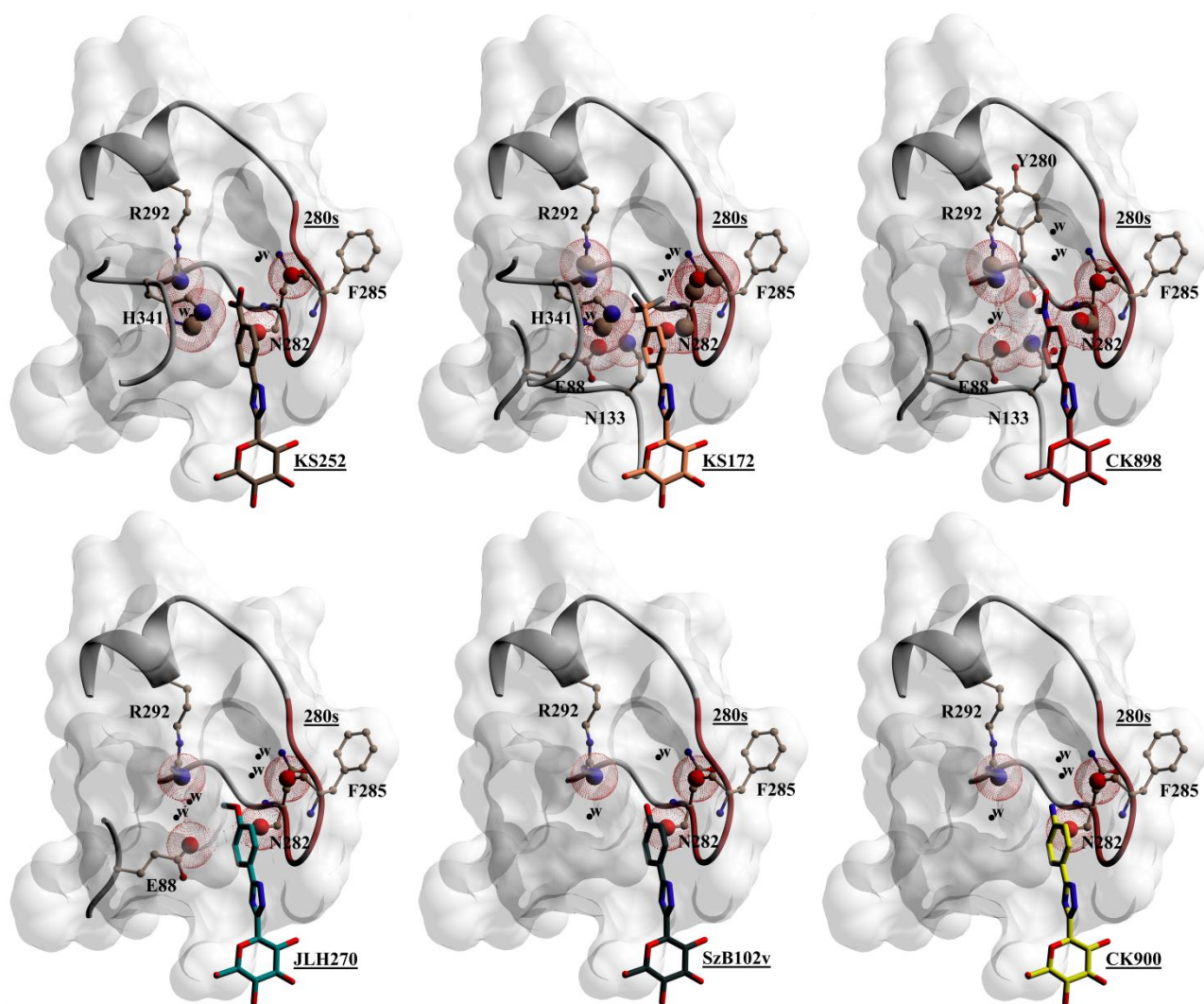


**Figure 4.** Diagrams of the binding of **KS252**, **KS172**, **CK898**, **JLH270**, **SzB102v**, and **CK900** at the active site of rmGPb. Van der Waals interacting protein atoms are shown bigger and in meshed spheres. Water molecules are labelled with W.

In total, **KS252**, **KS172**, **CK898**, **JLH270**, **SzB102v**, and **CK900** engage in 82, 79, 78, 76, 75, and 84 van der Waals interactions with protein residues at the active site of rmGPb, respectively. The phenyl group is involved in an extensive network of van der Waals interactions with protein residues Glu88, Asn282, Asn284, Phe285 and His341. In addition all six inhibitors are involved in  $\pi$ -cation interactions between their phenyl ring and the imidazole ring of His341. These interactions have been also observed with inhibitors **2a** and **2d** and were the source of the significant potency displayed by these compounds [18].

Focusing on the interactions of the *para* substituent reveals the structural basis of their significant differences in inhibitory potency. Thus, in **KS252** ( $K_i=637.4 \mu\text{M}$ ) this group ( $-\text{COO}^-$ ) does not form

any hydrogen bond interactions with protein residues in the active site (Table 3) and is only involved in 7 van der Waals interactions. The carboxylate of **KS252** is also at a salt bridge distance from Arg292 and His341 side chains (4.3 and 4.4 Å, respectively). In **KS172** ( $K_i=53.3 \mu\text{M}$ ) the  $\text{CF}_3$  group forms four halogen bonds with Asn282, Phe285 and Arg292 and is involved in 11 van der Waals interactions (Table 4). Halogen bond interactions have led to significant increment of the inhibitory potency of glycogen phosphorylase inhibitors in previous studies [44, 45]. The  $-\text{NO}_2$  group of **CK898** ( $K_i=32.7 \mu\text{M}$ ) is involved in a hydrogen bond with Arg292 and 8 van der Waals interactions. The  $-\text{OCH}_3$  group of **JLH270** ( $K_i=5.25 \mu\text{M}$ ) is not involved in any hydrogen bond interactions and forms 5 van der Waals interactions with Glu88, Asn282, Ph285 and Arg292 (Table 4). Finally, the hydroxyl group of **SzB102v** ( $K_i=3.66 \mu\text{M}$ ) and the  $-\text{NH}_2$  group of **CK900** ( $K_i=0.427 \mu\text{M}$ ) are not involved in any direct hydrogen bond interaction with protein residues and each one participates in only three van der Waals interactions with Asn282, Ph285 and Arg292 (Table 4).

<b>Table 4.</b> van der Waals interactions of the p-group of the six inhibitors with rmGPb in the crystal		
<b>Inhibitor</b>	<b>p-group atoms</b>	<b>Van der Waals interactions</b>
<b>KS252</b>	C12	Asn282(O); His341 (CE1,NE2); Phe285 (O); Wat182 (O); Wat195 (O)
	O13	His341 (NE2); Phe285 (O)
	O14	Arg292 (NH2); Asn282 (O); Wat182 (O)
<b>KS172</b>	C12	Asn282 (O); Phe285 (O); Wat195 (O); Wat182 (O); Wat362 (O)
	F13	His341(CE1,NE2); Arg292(CZ); Wat182 (O); Wat195 (O)
	F14	Asn282 (C,CB); Phe285 (C); Wat362 (O)
	F15	Glu88 (OE2); Asn133 (ND2); Arg292 (NH2); Wat195 (O)
<b>CK898</b>	N12	Wat195 (O); Wat182 (O)
	O13	Asn282 (O); Arg292 (CZ); Phe285 (O), Wat196 (O)
	O14	Glu88 (OE2); Asn282 (C); Asn133 (ND2); Tyr280 (O); Wat195 (O); Wat182 (O)
<b>JLH270</b>	O12	Asn282 (O); Phe285 (O); Wat362 (O); Wat182 (O)
	C13	Asn282 (O); Glu88 (OE2); Arg292 (NH2); Wat288 (O); Wat195(O); Wat184 (O)
<b>SzB102v</b>	O12	Ans282 (O); Arg292 (NH2); Phe285 (O); Wat195 (O); Wat182 (O)
<b>CK900</b>	N12	Asn282 (O); Arg292 (NH2); Phe285 (O); Wat182 (O); Wat195 (O); Wat632 (O)

It seems that there is no direct relation between the number of contacts and the  $K_i$  values, but there is some relation between the type of contacts (i.e. hydrogen bonds, van der Waals) and the strength of binding. Thus, the proximity and the interactions of polar atoms from protein residues and water molecules to C12 of **KS252** and **KS172** (Table 4) may provide an unfavorable determinant in the binding so that the  $K_i$  of these inhibitors are the worse among the six inhibitors studied. These inter-

actions are not compensated by the interactions of O13 and O14 in **KS252** with positive polar atoms (Arg292-NH2 and His341-NE2) since they also interact with negative polar atoms (Asn282-O and Phe285-O). The halogen bond interactions of **KS172** (Table 3) significantly compensate for these unfavorable interactions and hence the  $K_i$  of **KS172** is almost 8 times lower than that of **KS252**. For **CK898** the interactions of the NO<sub>2</sub> group are with polar atoms (Table 4). The NO<sub>2</sub> group is also close to the carbonyl oxygen of the main chain of Asn282 (2.8 Å) a rather unfavorable interaction which influences negatively the  $K_i$  value of this inhibitor, which is only 1.6 times lower than that of **KS172**. Both **JLH270** and **SzB102v** are almost equipotent and share the same interactions with protein residues. These interactions are mostly polar-nonpolar for **JLH270** and polar-polar for **SzB102v**. There are not any polarity issues here and hence their  $K_i$  values are 6.2 and 8.9 times lower than that of **CK898**, respectively. However, the close proximity of two water molecules to C13 of **JLH270** may provide an unfavorable interaction influencing negatively its inhibitory potency. These water molecules within the active site are firmly bound and conserved and hence are an integral part of the structure. Finally, **CK900** is the most potent inhibitor of all six studied here since it seems that has only favorable polar-polar van der Waals interactions and an additional hydrogen bond interaction with the side chain of Asn284 (Table 3) leading to a  $K_i$  value 8.5 times lower than that of **SzB102v**. **CK900** is equipotent with **2a** that has a methyl group instead of an amine. Although the physicochemical nature of the two *para* substituents is totally different, the  $\beta$ -pocket is lined by both polar and nonpolar groups and this mixed character has presented opportunities for favorable interactions for both groups. Given the significant difference of the two substituent groups their equipotency was somehow unexpected suggesting that in every step of the inhibitor optimization process structural data are needed to guide it and provide the rationale for the next step.

In a previous study [46] the inhibitory potency of a series of ten N<sup>1</sup>-( $\beta$ -D-glucopyranosyl)-4-substituted benzoyl-ureas was assessed by kinetic and crystallographic methods. Some of these inhibitors had groups at the *para* position identical with the ones presented here (i.e. -H (**2a**), -CH<sub>3</sub> (**2d**), -OH (**SzB102v**), -NO<sub>2</sub> (**CK898**), -NH<sub>2</sub> (**CK900**), -OCH<sub>3</sub> (**JLH270**), and -COO<sup>-</sup> (**KS252**)).



Their  $K_i$  values for rmGPb were at the range of low  $\mu\text{M}$  (i.e. 4.6, 2.3, 6.3, 3.3, 6.0, 3.2, and 85.0  $\mu\text{M}$ , respectively) [46]. As it appears with the exception of the  $-\text{COO}^-$  group all other substitutions lead to almost equipotent compounds. This equipotency was not well correlated with structural data that showed significant differences in the interactions of each of the *para* substituents upon binding to rmGPb. Crystallographic analysis [46] showed that all these compounds induced a significant conformational change of the 280s loop compared to that of the compounds presented here (Fig. 5). It seems that the energy cost for the conformational change of 280s loop dictated almost entirely the inhibitory potency and therefore the different groups at the *para* position of the benzyl ring did not seem to have any effect at the inhibitor's potency. In contrast, the inhibitors presented here did not cause any significant conformational change of the 280s loop (or to any other part of the protein structure) and hence the effect of the *para* substituent groups on the inhibitory potency is significantly more profound and better correlated with structural data.

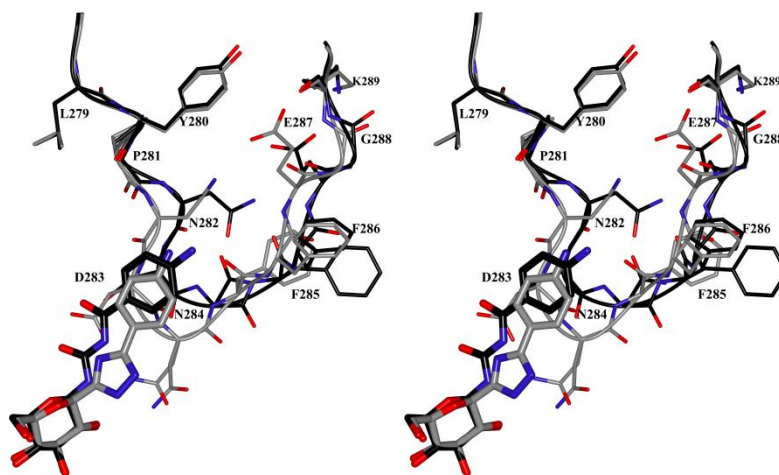


**Figure 5.** Stereo diagrams of the superposition of the complex structures rmGPb-CK900 in grey, and the corresponding urea analogue [46] in black.

The best *C*- $\beta$ -D glucopyranosyl triazole GP inhibitor reported thus far is **2b** which has a 2-naphthyl group (Table 1) and displays a  $K_i$  value of 0.172  $\mu\text{M}$  for the liver enzyme [18]. A recent study [16] suggested that this inhibitor targets beta cells and can be repurposed as agent to preserve beta cell function or even ameliorate beta cell dysfunction in different forms of diabetes. Comparative struc-

tural analysis of the rmGPb-**2b** and the rmGPb-**CK900** reveals that the two structures are very similar. In the rmGPb-**2b** complex the phenyl group of **2b** engages in van der Waals interactions with residues Asn282 (1), Asn284 (1), Phe285 (3), Arg292 (2), His341 (7), and Ala383 (1). In the rmGPb-**CK900** complex the *para* NH<sub>2</sub> group engages polar-polar interactions with the carbonyl oxygens of Asn282, Phe285 and the side chain of His341. Thus, although the *para* substituent of these two inhibitors is different in terms of polarity (hydrophobic vs hydrophilic) their interactions with protein residues lead to almost equipotent inhibition of these compounds ( $K_i$ s 0.172 and 0.427  $\mu$ M, respectively).

#### 4. Conclusions

The effect of six different groups, in size and hydrophobicity, in 3-(C- $\beta$ -D-glucopyranosyl)-5-phenyl-1,2,4-triazoles has been assessed by kinetic and X-ray crystallography methods. The best compound was the one with an amine with a  $K_i$  value of 430 nM for hIGPa. Structural analysis highlighted the essential components of the  $\beta$ -pocket within the GP active site revealing hydrophilic and hydrophobic regions which depending on the physicochemical characteristics of the inhibitor can either favor or impede inhibitor binding. However, comparison of the  $K_i$  values of the six inhibitors studied and their structural mode of binding revealed that the addition of the *para* group led to significant increments in potency (3-4 times) only when this group exploited hydrophilic or hydrophobic interactions within the  $\beta$ -pocket. Finding a group that will exploit both is the next challenge in the rational design of new GPis.

#### Acknowledgments

This work was supported in part by the Postgraduate Programmes “Biotechnology-Quality assessment in Nutrition and the Environment”, “Application of Molecular Biology-Molecular Genetics-Molecular Markers”, Department of Biochemistry and Biotechnology, University of Thessaly. Work at the Synchrotron Radiation Sources, MAX-lab, Lund, Sweden was supported from the EU FP7 Programme (FP7/2007-2013) under BioStruct-X (grant agreement N°283570). E.K. would like

to acknowledge financial support from the Hellenic State Scholarships Foundation and the action "Support of human research resources through doctoral research" funded by the "Operational Programme Education and Lifelong Learning" co-funded by the European Social Fund (ESF) and National Resources. Works in the Debrecen group received financial support from the projects OTKA CK77712 and PD105808 as well as GINOP-2.3.2-15-2016-00008 the latter funded by the EU and co-financed by the European Regional Development Fund.

## References

- [1] J.M. Hayes, A.L. Kantsadi, D.D. Leonidas, Natural products and their derivatives as inhibitors of glycogen phosphorylase: potential treatment for type 2 diabetes, *Phytochem. Rev.* 13(2) (2014) 471-498.
- [2] International, Diabetes, Federation, *IDF Diabetes Atlas, Seventh Edition*, Brussels, Belgium, 2015.
- [3] C.J. Bailey, Biguanides and NIDDM, *Diabetes Care* 15(6) (1992) 755-72.
- [4] C.J. Rhodes, Type 2 diabetes-a matter of beta-cell life and death?, *Science* 307(5708) (2005) 380-4.
- [5] T. Docsa, K. Czifrak, C. Huse, L. Somsak, P. Gergely, Effect of glucopyranosylidene-spirothiohydantoin on glycogen metabolism in liver tissues of streptozotocin-induced and obese diabetic rats, *Mol. Med. Report.* 4(3) (2011) 477-481.
- [6] N.G. Oikonomakos, Glycogen phosphorylase as a molecular target for type 2 diabetes therapy, *Curr. Protein. Pept. Sci.* 3(6) (2002) 561-86.
- [7] L. Somsak, K. Czifrak, M. Toth, E. Bokor, E.D. Chrysina, K.M. Alexacou, J.M. Hayes, C. Tiraidis, E. Lazoura, D.D. Leonidas, S.E. Zographos, N.G. Oikonomakos, New inhibitors of glycogen phosphorylase as potential antidiabetic agents, *Curr. Med. Chem.* 15(28) (2008) 2933-2983.
- [8] L. Somsák, E. Bokor, K. Czifrák, L. Juhász, M. Tóth, Carbohydrate Derivatives and Glycomimetic Compounds in Established and Investigational Therapies of Type 2 Diabetes Mellitus, in: M. Zimring (Ed.), *Topics in the Prevention, Treatment and Complications of Type 2 Diabetes*, InTech, 2011.
- [9] L. Somsak, Glucose derived inhibitors of glycogen phosphorylase, *Compt. Rend. Chim.* 14(2-3) (2011) 211-223.
- [10] T. Docsa, B. Marics, J. Nemeth, C. Huse, L. Somsak, P. Gergely, B. Peitl, Insulin sensitivity is modified by a glycogen phosphorylase inhibitor: glucopyranosylidene-spiro-thiohydantoin in streptozotocin-induced diabetic rats, *Curr. Top. Med. Chem.* 15(23) (2015) 2390-2394.
- [11] G.A. Stravodimos, B.A. Chetter, E. Kyriakis, A.L. Kantsadi, D.S. Chatzileontiadou, V.T. Skamnaki, A. Kato, J.M. Hayes, D.D. Leonidas, Phytogetic Polyphenols as Glycogen Phosphorylase Inhibitors: The Potential of Triterpenes and Flavonoids for Glycaemic Control in Type 2 Diabetes, *Curr. Med. Chem.* 24(4) (2017) 384-403.
- [12] D. Goyard, B. Konya, A.S. Chajistamatiou, E.D. Chrysina, J. Leroy, S. Balzarini, M. Tournier, D. Tusch, P. Petit, C. Duret, P. Maurel, L. Somsak, T. Docsa, P. Gergely, J.P. Praly, J. Azay-Milhau, S. Vidal, Glucose-derived spiro-isoxazolines are anti-hyperglycemic agents against type 2 diabetes through glycogen phosphorylase inhibition, *Eur. J. Med. Chem.* 108 (2016) 444-454.
- [13] L. Nagy, T. Docsa, M. Szanto, A. Brunyanszki, C. Hegedus, J. Marton, B. Konya, L. Virag, L. Somsak, P. Gergely, P. Bai, Glycogen Phosphorylase Inhibitor N-(3,5-Dimethyl-Benzoyl)-N'-(beta-D-Glucopyranosyl)Urea Improves Glucose Tolerance under Normoglycemic and Diabetic Conditions and Rearranges Hepatic Metabolism, *PLoS One* 8(7) (2013) e69420.
- [14] D.J. Baker, P.L. Greenhaff, A. MacInnes, J.A. Timmons, The experimental type 2 diabetes therapy glycogen phosphorylase inhibition can impair aerobic muscle function during prolonged contraction, *Diabetes* 55(6) (2006) 1855-61.
- [15] D.J. Baker, J.A. Timmons, P.L. Greenhaff, Glycogen phosphorylase inhibition in type 2 diabetes therapy - A systematic evaluation of metabolic and functional effects in rat skeletal muscle, *Diabetes* 54(8) (2005) 2453-2459.

- [16] L. Nagy, J. Marton, A. Vida, G. Kis, E. Bokor, S. Kun, M. Gonczi, T. Docsa, A. Toth, M. Antal, P. Gergely, B. Csoka, P. Pacher, L. Somsak, P. Bai, Glycogen phosphorylase inhibition improves beta cell function, *Br. J. Pharmacol.* 175 (2018) 301-319.
- [17] A.L. Kantsadi, E. Bokor, S. Kun, G.A. Stravodimos, D.S. Chatzileontiadou, D.D. Leonidas, E. Juhasz-Toth, A. Szakacs, G. Batta, T. Docsa, P. Gergely, L. Somsak, Synthetic, enzyme kinetic, and protein crystallographic studies of C-beta-d-glucopyranosyl pyrroles and imidazoles reveal and explain low nanomolar inhibition of human liver glycogen phosphorylase, *Eur. J. Med. Chem.* 123 (2016) 737-745.
- [18] A.L. Kantsadi, G.A. Stravodimos, E. Kyriakis, D.S.M. Chatzileontiadou, T.G.A. Solovou, S. Kun, E. Bokor, L. Somsak, D.D. Leonidas, van der Waals interactions govern C-beta-d-glucopyranosyl triazoles' nM inhibitory potency in human liver glycogen phosphorylase, *J. Struct. Biol.* 199(1) (2017) 57-67.
- [19] D. Barford, J.W.R. Schwabe, N.G. Oikonomakos, K.R. Acharya, J. Hajdu, A.C. Papageorgiou, J.L. Martin, J.C.A. Knott, A. Vasella, L.N. Johnson, Channels at the Catalytic Site of Glycogen Phosphorylase-B - Binding and Kinetic-Studies with the Beta-Glycosidase Inhibitor D-Gluconohydroximo-1,5-Lactone N-Phenylurethane, *Biochemistry* 27(18) (1988) 6733-6741.
- [20] S. Kun, E. Bokor, G. Varga, B. Szocs, A. Pahi, K. Czifrak, M. Toth, L. Juhasz, T. Docsa, P. Gergely, L. Somsak, New synthesis of 3-(beta-D-glucopyranosyl)-5-substituted-1,2,4-triazoles, nanomolar inhibitors of glycogen phosphorylase, *Eur. J. Med. Chem.* 76 (2014) 567-79.
- [21] E.H. Fischer, E.G. Krebs, Muscle Phosphorylase-B, *Methods Enzymol.* 5 (1962) 369-373.
- [22] N.G. Oikonomakos, A.E. Melpidou, L.N. Johnson, Crystallization of pig skeletal phosphorylase b. Purification, physical and catalytic characterization, *Biochim. Biophys. Acta* 832(3) (1985) 248-56.
- [23] S. Saheki, A. Takeda, T. Shimazu, Assay of inorganic phosphate in the mild of pH range, suitable for measurement of glycogen phosphorylase activity, *Anal. Biochem.* 148 (1985) 277-281.
- [24] R.J. Leatherbarrow, *GrafFit Version 6.0*. Erithakus Software, Staines, UK., 2007.
- [25] K.M. Alexacou, A.C. Tenchiu Deleanu, E.D. Chrysinia, M.D. Charavgi, I.D. Kostas, S.E. Zographos, N.G. Oikonomakos, D.D. Leonidas, The binding of beta-d-glucopyranosyl-thiosemicarbazone derivatives to glycogen phosphorylase: A new class of inhibitors, *Bioorg. Med. Chem.* 18(22) (2010) 7911-22.
- [26] T.G. Battye, L. Kontogiannis, O. Johnson, H.R. Powell, A.G. Leslie, iMOSFLM: a new graphical interface for diffraction-image processing with MOSFLM, *Acta Crystallogr. D Biol. Crystallogr.* 67(Pt 4) (2011) 271-281.
- [27] CCP4, The CCP4 suite : programs for protein crystallography, *Acta Crystallogr. D* 50 (1994) 760-763.
- [28] P.R. Evans, G.N. Murshudov, How good are my data and what is the resolution?, *Acta Crystallogr. D Biol. Crystallogr.* 69(Pt 7) (2013) 1204-1214.
- [29] G.N. Murshudov, P. Skubak, A.A. Lebedev, N.S. Pannu, R.A. Steiner, R.A. Nicholls, M.D. Winn, F. Long, A.A. Vagin, REFMAC5 for the refinement of macromolecular crystal structures, *Acta Crystallogr. D Biol. Crystallogr.* 67(Pt 4) (2011) 355-67.
- [30] A.A. Lebedev, P. Young, M.N. Isupov, O.V. Moroz, A.A. Vagin, G.N. Murshudov, JLigand: a graphical tool for the CCP4 template-restraint library, *Acta Crystallogr. D Biol. Crystallogr.* 68(Pt 4) (2012) 431-40.
- [31] P. Emsley, K. Cowtan, Coot: model-building tools for molecular graphics, *Acta Crystallogr. D Biol. Crystallogr.* 60(Pt 12 Pt 1) (2004) 2126-2132.
- [32] R.P. Joosten, F. Long, G.N. Murshudov, A. Perrakis, The PDB\_REDO server for macromolecular structure model optimization, *IUCrJ* 1 (2014) 213-220.
- [33] V.B. Chen, W.B. Arendall, 3rd, J.J. Headd, D.A. Keedy, R.M. Immormino, G.J. Kapral, L.W. Murray, J.S. Richardson, D.C. Richardson, MolProbity: all-atom structure validation for macromolecular crystallography, *Acta Crystallogr. D Biol. Crystallogr.* 66(Pt 1) (2010) 12-21.
- [34] M.D. Winn, C.C. Ballard, K.D. Cowtan, E.J. Dodson, P. Emsley, P.R. Evans, R.M. Keegan, E.B. Krissinel, A.G. Leslie, A. McCoy, S.J. McNicholas, G.N. Murshudov, N.S. Pannu, E.A. Potterton, H.R. Powell, R.J. Read, A. Vagin, K.S. Wilson, Overview of the CCP4 suite and current developments, *Acta Crystallogr. D Biol. Crystallogr.* 67(Pt 4) (2011) 235-242.
- [35] S. McNicholas, E. Potterton, K.S. Wilson, M.E. Noble, Presenting your structures: the CCP4mg molecular-graphics software, *Acta Crystallogr. D Biol. Crystallogr.* 67(Pt 4) (2011) 386-94.
- [36] V.L. Rath, M. Ammirati, P.K. LeMotte, K.F. Fennell, M.N. Mansour, D.E. Danley, T.R. Hynes, G.K. Schulte, D.J. Wasilko, J. Pandit, Activation of human liver glycogen phosphorylase by alteration of the secondary structure and packing of the catalytic core, *Mol. Cell* 6(1) (2000) 139-148.
- [37] A.L. Kantsadi, S. Manta, A.M. Psarra, A. Dimopoulou, C. Kiritsis, V. Parmenopoulou, V.T. Skamnaki, P. Zoumpoulakis, S.E. Zographos, D.D. Leonidas, D. Komiotis, The binding of C5-alkynyl and

- alkylfurano[2,3-d]pyrimidine glucopyranonucleosides to glycogen phosphorylase b: synthesis, biochemical and biological assessment, *Eur. J. Med. Chem.* 54 (2012) 740-9.
- [38] J.L. Martin, L.N. Johnson, S.G. Withers, Comparison of the binding of glucose and glucose 1-phosphate derivatives to T-state glycogen phosphorylase b, *Biochemistry* 29(48) (1990) 10745-57.
- [39] J.L. Martin, K. Veluraja, K. Ross, L.N. Johnson, G.W.J. Fleet, N.G. Ramsden, I. Bruce, M.G. Orchard, N.G. Oikonomakos, A.C. Papageorgiou, D.D. Leonidas, H.S. Tsitoura, Glucose analogue inhibitors of glycogen phosphorylase: The design of potential drugs for diabetes, *Biochemistry (USA)* 30(42) (1991) 10101-10116.
- [40] C.J.F. Bichard, E.P. Mitchell, M.R. Wormald, K.A. Watson, L.N. Johnson, S.E. Zographos, D.D. Koutra, N.G. Oikonomakos, G.W.J. Fleet, Potent Inhibition of Glycogen-Phosphorylase by a Spirohydantoin of Glucopyranose - First Pyranose Analogs of Hydantocidin, *Tetrahedron Lett.* 36(12) (1995) 2145-2148.
- [41] E.D. Chrysina, M.N. Kosmopoulou, C. Tiraidis, R. Kardakaris, N. Bischler, D.D. Leonidas, Z. Hadady, L. Somsak, T. Docsa, P. Gergely, N.G. Oikonomakos, Kinetic and crystallographic studies on 2-(beta-D-glucopyranosyl)-5-methyl-1, 3, 4-oxadiazole, -benzothiazole, and -benzimidazole, inhibitors of muscle glycogen phosphorylase b. Evidence for a new binding site, *Protein Sci.* 14(4) (2005) 873-88.
- [42] M. Gregoriou, M.E. Noble, K.A. Watson, E.F. Garman, T.M. Krulle, C. de la Fuente, G.W. Fleet, N.G. Oikonomakos, L.N. Johnson, The structure of a glycogen phosphorylase glucopyranose spirohydantoin complex at 1.8 Å resolution and 100 K: the role of the water structure and its contribution to binding, *Protein Sci.* 7(4) (1998) 915-27.
- [43] N.G. Oikonomakos, V.T. Skamnaki, E. Osz, L. Szilagy, L. Somsak, T. Docsa, B. Toth, P. Gergely, Kinetic and crystallographic studies of glucopyranosylidene spirothiohydantoin binding to glycogen phosphorylase B, *Bioorg. Med. Chem.* 10(2) (2002) 261-268.
- [44] A.L. Kantsadi, J.M. Hayes, S. Manta, V.T. Skamnaki, C. Kiritsis, A.M.G. Psarra, Z. Koutsogiannis, A. Dimopoulou, S. Theofanous, N. Nikoleousakos, P. Zoumpoulakis, M. Kontou, G. Papadopoulos, S.E. Zographos, D. Komiotis, D.D. Leonidas, The s-Hole Phenomenon of Halogen Atoms Forms the Structural Basis of the Strong Inhibitory Potency of C5 Halogen Substituted Glucopyranosyl Nucleosides towards Glycogen Phosphorylase b, *ChemMedChem* 7(4) (2012) 722-732.
- [45] S. Manta, A. Xipnitou, C. Kiritsis, A.L. Kantsadi, J.M. Hayes, V.T. Skamnaki, C. Lamprakis, M. Kontou, P. Zoumpoulakis, S.E. Zographos, D.D. Leonidas, D. Komiotis, 3'-Axial CH<sub>2</sub>OH Substitution on Glucopyranose does not Increase Glycogen Phosphorylase Inhibitory Potency. QM/MM-PBSA Calculations Suggest Why, *Chem. Biol. Drug Des.* 79(5) (2012) 663-673.
- [46] V. Nagy, N. Felfoldi, B. Konya, J.P. Praly, T. Docsa, P. Gergely, E.D. Chrysina, C. Tiraidis, M.N. Kosmopoulou, K.M. Alexacou, M. Konstantakaki, D.D. Leonidas, S.E. Zographos, N.G. Oikonomakos, S. Kozmon, I. Tvaroska, L. Somsak, N-(4-Substituted-benzoyl)-N'-(beta-D-glucopyranosyl)ureas as inhibitors of glycogen phosphorylase: Synthesis and evaluation by kinetic, crystallographic, and molecular modelling methods, *Bioorg. Med. Chem.* 20(5) (2012) 1801-1816.